Biosensors and Bioelectronics 97 (2017) 164–168

Contents lists available at ScienceDirect

Biosensors and Bioelectronics

journal homepage: www.elsevier.com/locate/bios

A smartphone-based chloridometer for point-of-care diagnostics of cystic fibrosis

Chenji Zhang[a,1], Jimin P. Kim[b,1], Michael Creer[c], Jian Yang[b,*], Zhiwen Liu[a,*]

[a] Department of Electrical Engineering, Material Research Institutes, The Pennsylvania State University, University Park, PA 16802, USA
[b] Department of Biomedical Engineering, Materials Research Institutes, the Huck Institutes of Life Sciences, The Pennsylvania State University, University Park, PA 16802, USA
[c] Department of Pathology, College of Medicine, The Pennsylvania State University, Hershey, PA 17033, USA

ARTICLE INFO

Keywords:
Fluorescence
Sensor
Optics
Chloride
Point-of-care
Cystic fibrosis

ABSTRACT

Chloride in sweat is an important diagnostic marker for cystic fibrosis (CF), but the implementation of point-of-care systems for diagnosis is hindered by the prohibitive costs of existing chloride sensors. To enable low cost diagnostic solutions, we recently established a citrate-derived synthesis platform for the development of new fluorescence sensors with high selectivity for chloride. As a next step, we herein designed a smartphone operated chloridometer that optimizes the analytical performance of the citrate-derived sensor materials for the detection of chloride in sweat. The sensor material demonstrated a wide linear range of 0.8–200 mM chloride and a diffusion-limited response time; sweat chloride levels corresponded to measurable changes in fluorescence emission that was captured by a smartphone. Clinical validation was performed with sweat from individuals with and without CF, demonstrating convenient sweat diagnostics with reliable detection of cystic fibrosis. To our knowledge, this is the first clinical study of a smartphone-based chloride sensor, paving the way for point-of-care diagnostic systems for CF.

1. Introduction

Chloride is an essential electrolyte that maintains homeostasis within the body; thus evidence of various conditions and diseases can be presented in the chloride levels of biological fluids. For example, cystic fibrosis (CF) is a genetic multi-organ disease caused by a defective transmembrane ion regulator gene presented not only in the lungs and pancreas, but also in sweat glands such that elevated sweat chloride (> 60 mM) is the primary diagnostic criteria for CF (Watanabe et al., 2009; Golubnitschaja, 2009; Blythe and Farrell, 1984). Likewise, chloride levels in urine and serum are respectively used for the screening of metabolic alkalosis and Addison's disease (Watanabe et al., 2009). Hence diagnostics provided at the point-of-care would facilitate early detection of such diseases and enable timely treatments (Golubnitschaja, 2009). Early diagnosis of CF, for instance, has been shown to prevent serious malnutrition and promote long-term growth of affected infants (Blythe and Farrell, 1984; Farrell et al., 1993, 2001; Kosorok et al., 1996; Lai et al., 1998). Moreover, there is a significant demand for low-cost chloridometers not only for diagnostic purposes, but also for routine personal health monitoring (Dam et al., 2016; Fidler et al., 2016; Geddes, 2001). For instance, sweat chloride is a predictive pharmacodynamic biomarker of pulmonary improvement in the treatment of cystic fibrosis, enabling tracking of systemic response and patient compliance through routine monitoring of sweat chloride (Fidler et al., 2016). Regular monitoring of sweat chloride can also assess dehydration in athletes (Dam et al., 2016).

Despite the clinical importance of sweat chloride as a diagnostic marker, the transition of chloride sensors from laboratories to the point-of-care has been hindered by prohibitive costs. Chloridometers based on ion-selective electrodes (ISE) typically cost several thousand dollars and suffer from significant interference from nitrates and bicarbonates, while automated analyzers based on coulometry or colorimetry can cost in the tens of thousands (Bray et al., 1977; Lynch et al., 2000; McClatchey, 2002). Consequently, a wide-scale survey of about 400 clinical labs revealed that the determination of sweat chloride for the diagnosis of CF was performed with manual titration in almost 70% of labs, while automated analyzers were utilized in less than 7% (LeGrys, 2001). Manual titration with mercuric nitrate is time consuming and prone to technical error, leading to rates of misdiagnosis as high as 15% (Lezana et al., 2003; LeGrys et al., 2000; Shwachman and Antonowicz, 1962; Rosenstein et al., 1978). Thus there is an urgent need for new point-of-care diagnostic tools for sweat

* Corresponding authors.
E-mail addresses: jxy30@psu.edu (J. Yang), zliu@psu.edu (Z. Liu).
[1] These two authors contributed equally.

http://dx.doi.org/10.1016/j.bios.2017.05.048
Received 10 March 2017; Received in revised form 23 May 2017; Accepted 26 May 2017
Available online 27 May 2017
0956-5663/

chloride that can be readily translated into clinical settings as well as for routine personal health monitoring.

To meet the demand for convenient sweat diagnostics, our unique approach is to design a smartphone operated fluorometer equipped with a novel fluorescent chloride sensor such that chloride levels correspond to measurable changes in fluorescence emission. The wide availability of smartphones makes them an attractive mode of computation and communication in the design of point-of-care diagnostic systems, enabling convenient data sharing and management. Moreover, fluorescence-based sensing methods offer high sensitivity, rapid response kinetics and low technical complexity for end users (Lakowicz, 2013). Although the union of fluorescence sensing and low-cost optics offers powerful advantages, the success of such fluorescence-based devices has been limited thus far by the lack of viable sensor materials. Existing fluorescence chloride sensors, including quinolinium-based dyes and more recent turn-on sensors, suffer from severe drawbacks such as narrow linear range (< 10–20 mM), poor aqueous sensing (requiring organic stabilizers), costly syntheses, and poor selectivity among common ions (e.g. acetate, carbonate, phosphate) (Geddes et al., 2001; Lakowicz et al., 2013; Porel et al., 2013; Riis-Johannessen et al., 2010; Watt et al., 2015). To overcome these challenges, we recently established a citrate-derived synthesis platform for the versatile design of new fluorescence chloride sensors with improved sensing properties. As a next step, we herein develop a smartphone-based device that optimizes the performance of our citrate-derived sensor materials to enable point-of-care sweat diagnostics for cystic fibrosis. To evaluate clinical performance, we defined quantitative metrics in two aspects: (1) analytical validation with sweat controls according to the College of American Pathologists guidelines, and (2) clinical validation with sweat from individuals with or without CF using a rigorous Bland & Altman approach.

2. Experimental

2.1. Synthesis

Citrate-based fluorescent sensors are synthesized via a one-pot reaction of citric acid and a primary amine in water. In this work, CA-Cysteine was synthesized with equimolar ratios of citric acid (0.01 mol) and L-cysteine (0.01 mol) in a flask, reacted at 140 °C for 30 min, and terminated by addition of 10 mL of DI water. Purification was performed through two cycles of crystallization in DI water and freeze-drying. Chemical structures were previously characterized by HPLC-ESI-MS, FTIR, ^{1}H and ^{13}C NMR studies (Xie et al., 2017; Yang et al., 2009).

2.2. Device fabrication

A smartphone operated chloridometer was designed to integrate our citrate-derived chloride sensor into a convenient point-of-care device. The chloridometer works as a smartphone accessory that is equipped with an ultraviolet (UV) light emitting diode (LED) light source to generate fluorescence from our sensor material, which is collected and measured by the smartphone camera for quantitative determination of chloride from prepared samples. The UV-LED excitation light source (365 nm excitation, maximum 1 W output power) was soldered onto a printed circuit board, adjoined to an aluminum block for heat dissipation, and powered by a 9 V battery. To maintain a stable operating temperature and reliable device performance, a 7-ohm high power resistor was used to control the voltage and current applied to the LED, limiting the applied voltage to 4.1 V and current to 700 mA as specified by the manufacturer. An HTC One M9 smartphone was used for all experiments, with its camera optimized with an exposure time of 10 ms, ISO of 100, and focus at near field to capture a dng raw image of the cuvette sample holder placed very close to the camera. Our device design accommodates most types of smartphones given that the camera parameters (e.g. white balance, gain level, exposure time, and focal lengths) are fixed during the calibration curve and sample measurement. The fluorescence intensity of each measurement was determined by the summation of the total pixel values of the captured fluorescence pattern. This blue fluorescence was collected by the smartphone camera from a direction orthogonal to that of the excitation light to reduce UV light breakthrough. In addition, a 441.6 nm band-pass filter was used (L441.6-10 Ø1" Laser Line Filter) to completely remove the excitation light since the fluorescence emission wavelength of CA-Cysteine is maximal at 441 nm. The device was 3D printed (via Solidoodle) out of black acrylonitrile-butadiene-styrene plastic.

2.3. Sample preparation and measurement

To perform measurement, a chloride sample (1 mL) was diluted with CA-Cysteine (1 mL) and sulfuric acid (0.5 mL) in a quartz cuvette. Sensor concentration was kept fixed throughout all experiments at a final concentration of 11.6 μM (corresponding to an absorbance of 0.1 optical density at 365 nm), along with a final concentration of 0.16 M sulfuric acid and a final sample dilution factor of 2.5x. CA-Cysteine is a fluorescent small molecule that emits a strong blue fluorescence which is attenuated by the presence of chloride ions. An acidic solution allows protonation of the sensor's carboxyl groups in order to maintain reliable performance, a condition that can be met with mildly acidic 2% citric acid solutions, lower than found in orange juice (Kim et al., 2017). For this study, however, we utilized sulfuric acid to minimize any buffering effects from patient sweat that may alter the pH condition. A calibration curve was obtained by capturing fluorescence intensity at various chloride concentrations (0, 5, 10, 15, and 20 mM sodium chloride).

2.4. Clinical evaluation and statistical analysis

Sweat collection was performed at a clinic via standard pilocarpine iontophoresis, in which sweat from the right arm was analyzed by mercuric nitrate titration by technicians in the clinical laboratory and sweat from the left arm was centrifuged and then analyzed by our smartphone-based device as described above. For statistical analysis, the intraclass correlation coefficient (ICC) computed by MedCalc™ and the Bland & Altman plot were used to assess correlation and agreement between the two measurement methods. The Bland & Altman plot is useful in identifying systematic errors and outliers, where the mean difference is the estimated bias, and its 1.96 SD computes the 95% limit of agreement for the comparison of methods.

3. Results and discussion

3.1. Citrate-derived chloride sensors

In clinical measurements, sensor materials are expected to perform well in many different biological fluids and are often exposed to a broad analytical range. Chloride sensing is generally challenging in this respect, given that physiological chloride levels vary from 20 mM (sweat), 100 mM (CF sweat, serum), to over 200 mM (urine), among the highest for biomolecules (Sloan et al., 1984). To address this challenge, we have recently reported a citrate-derived synthesis platform for the design of new fluorescence chloride sensors based on a facile and low-cost reaction of citrate and a primary (Kim et al., 2017). The resulting family of chloride sensors possessed versatile sensing properties that can be tailored to suit the mean and range of various clinical tests such as sweat, urine, and serum analyses.

Herein we reacted citric acid and L-cysteine at 140 °C in water to synthesize a fluorescent molecular sensor, CA-Cysteine (Fig. 1A). We selected CA-Cysteine among other sensors due to its low cost, high chloride selectivity (Fig. 1C), and reliable performance in a broad

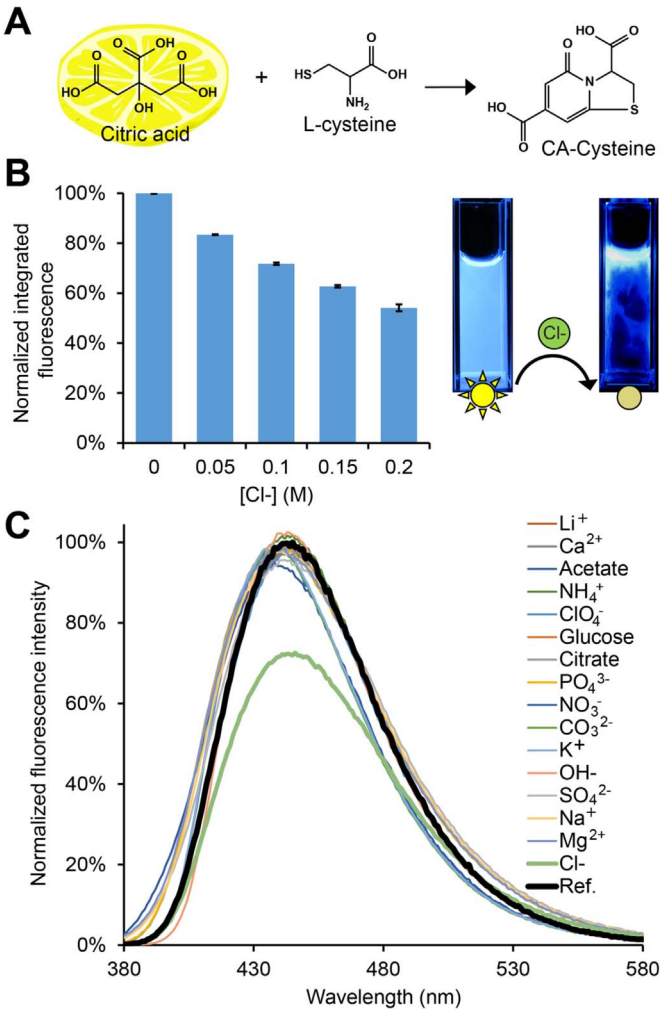

Fig. 1. (A) Synthesis of a citrate-derived chloride sensor, CA-Cysteine. (B) Linear range of chloride detection from quenching of CA-Cysteine fluorescence intensity. (C) CA-Cysteine quenching efficiency, showing chloride selectivity against common ions (0.1 M for all).

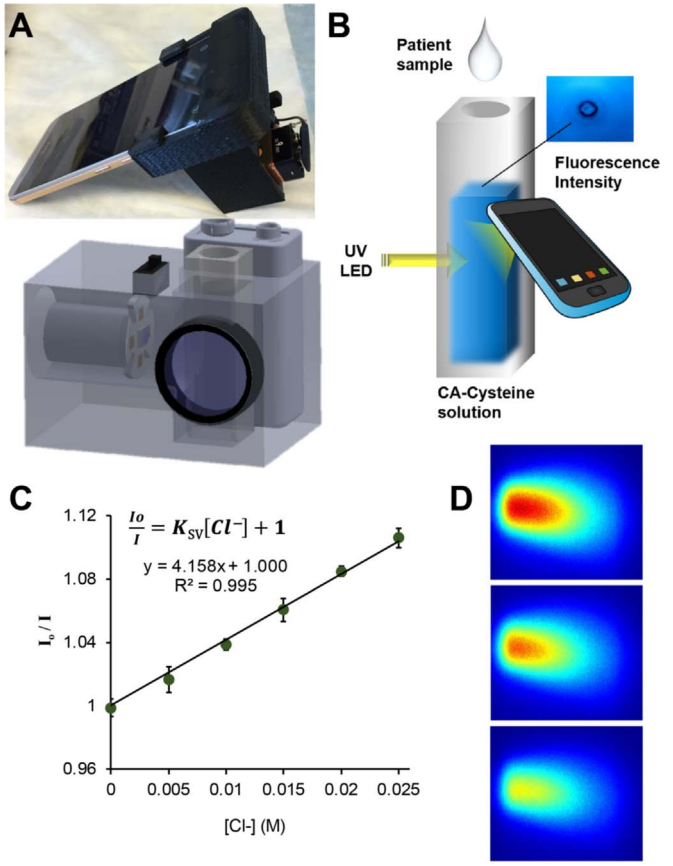

Fig. 2. (A-B) Photo and schematic diagram of the chloridometer system. (C) Calibration curve obtained by the Stern-Volmer relation to linearize fluorescence quenching rates (I_0/I) over chloride concentration to determine the K_{SV} (slope). (D) Raw images of CA-Cysteine fluorescence captured by a smartphone camera in the presence of increasing chloride concentrations.

analytical range (Fig. 1B). CA-Cysteine displayed a detection limit of 0.8 mM for chloride (Kim et al., 2017), maintaining an impressive linearity up to 200 mM (Fig. 1B) in fluorescence intensity signals. In contrast, existing chloride sensors including quinolinium-based dyes (Geddes, 2001; Geddes et al., 2001; Verkman, 1990) and various turn-on sensors (Porel et al., 2013; Riis-Johannessen et al., 2010; Watt et al., 2015) have higher sensitivities (K_{SV} > 200 M^{-1}) that are better suited for sub-micromolar chloride detection, which has few real world applications. For instance, a recently reported chloride analyzer based on N-[ethoxycarbonylmethyl]-6-methoxy-quinolinium (MQAE) displayed a non-linear response to saline chloride levels above 20 mM accompanied by significant loss of sensitivity (Wang et al., 2012), along with prohibitive material costs ($197/100 mg for MQAE, Thermo Fisher Scientific, 2016) that would deter routine health applications.

The seamless integration of a sensor material into fluorescence-based diagnostic systems relies on several key fluorescence properties that may enhance performance of optical devices. CA-Cysteine exhibited a strong blue fluorescence and favorable properties such as high quantum yield (81%), long lifetimes (10 ns), and exceptional photostability compared to commercial chloride sensors (Kim et al., 2017). In the design of fluorescence-based devices, high quantum yields would improve the signal-to-noise ratio while high photostability would enable reliable serial measurements. Moreover, the solvent- and catalyst-free synthesis scheme involving simple monomers granted cost-efficiency and nontoxicity (cytocompatibility up to 10.3 mM) (Kim et al., 2017) to our sensor material for safe handling procedures, whereas colorimetric chloridometers often utilize toxic reagents such as mercuric nitrate, mercuric thiocynate, or silver chromate.

3.2. Smartphone-operated chloride measurement

To integrate our citrate-derived chloride sensor into a point-of-care device, we designed a smartphone operated chloridometer equipped with an ultraviolet LED to generate fluorescence signals from CA-Cysteine, which is then captured by the smartphone camera. A schematic diagram and photo of the chloridometer system are shown in Fig. 2A-B. In detail, analyte recognition and signal transduction occur via fluorescence quenching mechanisms, in which the presence of chloride in a solution of CA-Cysteine leads to non-radiative relaxation of the excited fluorophore, resulting in visible attenuation of fluorescence (Kim et al., 2017). Next, signal processing is performed by summation of the total pixel values of the captured fluorescence image to quantify the fluorescence intensity of each measurement (Fig. 2D). A calibration curve (Fig. 2C) was then established by linearizing fluorescence quenching effects according to the Stern Volmer equation:

$$\frac{I_0}{I} = K_{SV}[Cl^-]+1 \quad (1)$$

where I_0 is the unquenched fluorescence intensity of CA-Cysteine, I is the quenched intensity at [Cl^-], and K_{SV} represents the chloride sensitivity of the sensor. Relative standard deviations in 0, 5, 10, 15, 20, and 25 mM Cl^- measured in triplicates were 0.53%, 0.81%, 0.32%, 0.70%, 0.29%, and 0.56% respectively. Finally, patient sweat samples

were prepared in our sensor solution, and the degree of fluorescence quenching was compared to the calibration curve to determine sweat chloride levels. As sweat is composed of numerous electrolytes that may interfere with chloride readings, we also performed a systematic investigation among common mono- and polyatomic ions and found that the environment sensitivity of CA-Cysteine fluorescence was limited to heavy halides (Kim et al., 2017), of which only chloride was deemed clinically relevant since physiological bromide and iodide are typically less than 40 μM and 1.6 μM respectively.

3.3. Clinical evaluation

Cystic fibrosis is a multi-organ disease caused by mutations in the CF transmembrane conductance regulator (CFTR) gene, conferring abnormal regulation of chloride by epithelial cells (Bush, 2006). Although CF typically affects lung or pancreatic function, evidence of CFTR dysfunction is also presented along sweat glands. In fact, the sweat chloride test is the gold standard for the diagnosis of CF, as patients homozygous for the CF gene have sweat chloride concentrations above 60 mM (Mishra et al., 2005; Scriver and Stanbury, 1989). To evaluate our smartphone-based device as a sweat diagnostics system for cystic fibrosis, we established quantitative metrics to define success in two aspects: (1) analytical validation with sweat controls according to College of American Pathologists guidelines, and (2) clinical validation with sweat from 10 individuals with or without CF using a Bland & Altman approach.

We performed analytical validation for sweat diagnostics using artificial sweat controls. Sweat controls (Quantimetrix, USA) simulate the human sweat at three levels, where QC-1 represents sweat of healthy individuals, while QC-2 and QC-3 represent the lower and upper ends of CF sweat respectively. Three replicates of each sweat control were prepared and analyzed based on the above protocol. QC-1 was measured at 21 ± 5.6 mM, QC-2 at 55 ± 3.6 mM, and QC-3 at 103 ± 7.4 mM, compared to the respective reference values of 23 mM, 51 mM, and 106 mM as obtained by Quantimetrix. The measured results agreed well with the reference values, obtaining ranges well within the evaluation criteria of ± 10.0 mM/L or 15% (whichever is greater) set by the College of American Pathologists (CAP) Laboratory Accreditation Program (LeGrys et al., 2000), and thus validating our smartphone-based chloridometer as a new sweat test method for the diagnosis of CF. Sources of error contributing to measurement variability include fluctuations in the excitation light source, which may be mitigated in future prototypes with a photodiode or by utilizing a second camera on the smartphone as self-reference to calibrate the excitation power.

Lastly, we performed clinical validation of our device with sweat from 5 healthy and 5 CF individuals to evaluate performance in the detection of cystic fibrosis. Sweat from the right arm was analyzed by mercuric nitrate titration (reference method) by clinical technicians and sweat from the left arm was analyzed by our smartphone-based device. There was excellent correlation between the two methods, as evidenced by an intraclass correlation coefficient (ICC) of 0.972 with a 95% confidence interval of (0.882, 0.9935) (Fig. 3A), which is considered a good-to-excellent level of reliability (Koo and Mae, 2016). The regression plot shows that CF and non-CF populations could be statistically identified with either method, even such that all CF individuals presented chloride above 60 mM while all non-CF individuals below 40 mM as per diagnostic criteria, meaning any disagreement between the two methods would not affect diagnostic results. The Bland & Altman plot showed a mean difference of −4.39 mM with a standard deviation of 14.6 mM, along with differences between methods within 29.2 mM at a 95% limit of agreement (Fig. 3B). This is an acceptable level of agreement between the two methods given that the typical range for sweat chloride measurements in different arms are ± 15 mM. We speculate that the negative bias (−4.39 mM) and the larger variability (± 14.6 mM) in clinical samples compared to sweat controls may be attributed to exfoliate particles absorbing incident light.

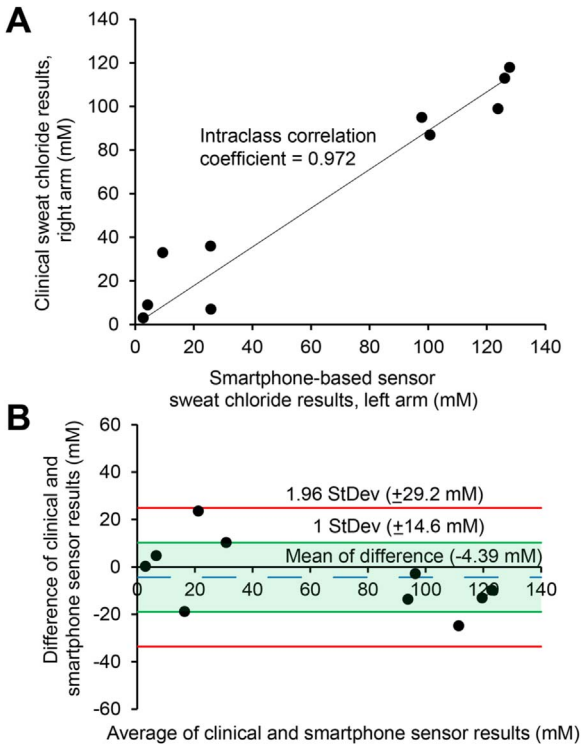

Fig. 3. Clinical validation of our smartphone-based chloridometer for CF diagnosis was implemented via (A) intraclass correlation coefficient measured by a regression plot and (B) agreement measured by a Bland & Altman plot against the clinical reference (standard mercuric nitrate titration).

4. Conclusion

In this work, we have achieved a sweat diagnostics system for cystic fibrosis by developing a low-cost smartphone based chloridometer equipped with a novel citrate-derived fluorescence sensor. The sensor material exhibited a broad linear range of 0.8–200 mM chloride, maintaining relative standard deviations below 1% throughout the detection range. Next, we have performed analytical and clinical validation of our device as a reliable and convenient optical sweat test method for the diagnosis of CF, which may significantly improve diagnostic accuracy by reducing technical complexity and human error in fast-paced clinical settings, and may have broader impact on the implementation of diagnostic tests in resource-scarce settings with limited access to sophisticated instrumentation (Yager et al., 2008). A major source of measurement error stemmed from fluctuations in the excitation light source power; future prototypes may incorporate a built-in self-reference along with a driver circuit to stabilize the LED light source and improve the system stability and reproducibility. Further, incorporating a miniaturized optical spectrometer may better resolve the fluorescence spectra, accounting for changes in spectral shape or wavelength shifts that may exist to improve sensor accuracy (Yang et al., 2010, 2011; Yu et al., 2014; Zhang et al., 2016).

Conflict of interest

Dr Yang and The Pennsylvania State University have a financial interest in Aleo BME, Inc. These interests have been reviewed by the University's Institutional and Individual Conflict of Interest Committees and are currently being managed by the University.

Acknowledgements

This work was supported in part by National Institutes of Health (NIH – United States) Awards (NIBIB EB012575, NCI CA182670) and by Vodafone Americas Foundation.

References

Blythe, S.A., Farrell, P.M., 1984. Clin. Biochem. 17, 277–283.
Bray, P., Clark, G., Moody, G., Thomas, J., 1977. Clin. Chim. Acta 80, 333–338.
Bush, A. (Ed.), 2006. Cystic Fibrosis in the 21st Century 34. Karger Medical and Scientific Publishers.
Dam, V., Zevenbergen, M., van Schaijk, R., 2016. Sens. Actuators B 236, 834–838.
Farrell, P., Gilbert-Barness, E., Bell, J., Gregg, R., Mischler, E., Odell, G., Shahidi, N., Robertson, I., Evans, J., 1993. Am. J. Med. Genet. 45, 725–738.
Farrell, P.M., Kosorok, M.R., Rock, M.J., Laxova, A., Zeng, L., Lai, H.-C., Hoffman, G., Laessig, R.H., Splaingard, M.L., 2001. Pediatrics 107, 1–13.
Fidler, M.C., Beusmans, J., Panorchan, P., Van Goor, F., 2016. J. Cyst. Fibros. 16, 41–44.
Geddes, C.D., 2001. Meas. Sci. Technol. 12, R53.
Geddes, C.D., Apperson, K., Karolin, J., Birch, D.J., 2001. Anal. Biochem. 293, 60–66.
Golubnitschaja, O., 2009. Croat. Med. J. 50, 596.
Koo, T.K., Mae, Y.L., 2016. J. Chiropr. Med. 15, 155–163.
Kim, J.P., Xie, Z., Creer, M., Liu, Z., Yang, J., 2017. Chem. Sci. 8, 550–558.
Kosorok, M.R., Wei, W.H., Farrell, P.M., 1996. Stat. Med. 15, 449–462.
Lai, H.-C., Kosorok, M.R., Sondel, S.A., Chen, S.-T., FitzSimmons, S.C., Green, C.G., Shen, G., Walker, S., Farrell, P.M., 1998. J. Pediatr. 132, 478–485.
Lakowicz, J.R., 2013. Principles of Fluorescence Spectroscopy. Springer Science & Business Media.
LeGrys, V.A., Burritt, M.F., Gibson, L.E., Hammond, K.B., Kraft, K., Rosenstein, B.J., 2000. Sweat testing: Sample Collection and Quantitative Analysis, Approved Guideline. National Committee for Clinical Laboratory Standards.
LeGrys, V.A., 2001. Arch. Pathol. Lab. Med. 125, 1420–1424.
Lezana, J.L., Vargas, M.H., Karam-Bechara, J., Aldana, R.S., Furuya, E., 2003. J. Cyst. Fibros. 2, 1–7.
Lynch, A., Diamond, D., Leader, M., 2000. Analyst 125, 2264–2267.
McClatchey, K.D. (Ed.), 2002. Clinical Laboratory Medicine. Lippincott Williams & Wilkins.
Mishra, A., Greaves, R., Massie, J., 2005. Clin. Biochem. Rev. 26, 135.
Porel, M., Ramalingam, V., Domaradzki, M.E., Young, V.G., Ramamurthy, V., Muthyala, R.S., 2013. Chem. Commun. 49, 1633–1635.
Riis-Johannessen, T., Schenk, K., Severin, K., 2010. Inorg. Chem. 49, 9546–9553.
Rosenstein, B., Langbaum, T., Gordes, E., Brusilow, S., 1978. JAMA 240, 1987–1988.
Scriver, C.R., Stanbury, J.B., 1989. The Metabolic Basis of Inherited Disease. McGraw-Hill, New York.
Shwachman, H., Antonowicz, I., 1962. Ann. N. Y. Acad. Sci. 93, 600–624.
Sloan, P.J., Beaver, G., Baxter, F.E., 1984. Clin. Chem. 30, 1705–1707.
Thermo Fisher Scientific. N.p., 2016.
Verkman, A.S., 1990. Am. J. Physiol. Cell. Physiol. 259, C375–C388.
Wang, J., Wu, X., Chon, C., Gonska, T., Li, D., 2012. Meas. Sci. Technol. 23, 025701.
Watanabe, S., Kimura, T., Suenaga, K., Wada, S., Tsuda, K., Kasama, S., Takaoka, T., Kajiyama, K., Takeda, M., Yoshikawa, H., 2009. J. Neurol. Sci. 285, 146–148.
Watt, M.M., Engle, J.M., Fairley, K.C., Robitshek, T.E., Haley, M.M., Johnson, D.W., 2015. Org. Biomol. Chem. 13, 4266–4270.
Xie, Z., Kim, J.P., Cai, Q., Zhang, Y., Guo, J., Dhami, R.S., Li, L., Kong, B., Su, Y., Schug, K.A., Yang, J., 2017. Acta Biomater. 50, 361–369.
Yager, P., Domingo, G.J., Gerdes, J., 2008. Annu. Rev. Biomed. Eng. 10, 107–144.
Yang, C., Shi, K., Edwards, P., Liu, Z., 2010. Opt. Express 18, 23529–23534.
Yang, C., Edwards, P., Shi, K., Liu, Z., 2011. Opt. Lett. 36, 2023–2025.
Yang, J., Zhang, Y., Gautam, S., Liu, L., Dey, J., Chen, W., Mason, R.P., Serrano, C.A., Schug, K.A., Tang, L., 2009. Proc. Natl. Acad. Sci. 106, 10086–10091.
Yu, H., Yafang, T., Cunningham, B., 2014. Anal. Chem. 86, 8805–8813.
Zhang, C., Cheng, G., Edwards, P., Zhou, M.-D., Zheng, S., Liu, Z., 2016. Lab Chip 16, 246–250.